Eur. Phys. J. D **4**, 365–372 (1998)

THE EUROPEAN PHYSICAL JOURNAL D

Classical dynamical simulation of spontaneous alloying

Y. Shimizu[1,a], S. Sawada[2,b], and K.S. Ikeda

[1] Department of Physics, Faculty of Science and Engineering, Ritsumeikan University, Noji-higashi 1-1-1, Kusatsu 525-8577, Japan
[2] Department of Electrical and Electronics Engineering, Faculty of Engineering, Kagoshima University, Kohrimoto 1-21-40, Kagoshima 890, Japan
[3] Department of Physics, Faculty of Science and Engineering, Ritsumeikan University, Noji-higashi 1-1-1, Kusatsu 525-8577, Japan

Received: 2 March 1998 / Revised: 21 May 1998 / Accepted: 28 May 1998

Abstract. "Spontaneous alloying" observed by Yasuda, Mori *et al.* for metallic small clusters is simulated using classical Hamiltonian dynamics. Very rapid alloying occurs homogeneously and cooperatively starting from the solid phase of the cluster if the heat of solution is negative and the size of cluster is less than a critical size. Analysis of 2D models reveals that the alloying rate obeys an Arrhenius-type law, which predicts the alloying time much less than *second* at room temperature. Evidences manifesting that the spontaneous alloying proceeds in the solid phase without melting are also presented. The simulation reproduces the essential features of the experiments.

PACS. 31.15.Qg Molecular dynamics and other numerical methods – 36.40.Sx Diffusion and dynamics of clusters

1 Introduction

An important feature of small clusters of atoms is that a relatively large fraction of atoms are on the surface and are easily deformable in relative positions. Small clusters thus suffer from anomalously large dynamical fluctuations. Indeed, several experimentalists observed that small metallic clusters undergo dynamical transitions among various shapes [1]. Coexistence of various quasi-equilibrium shapes implies that the phase space of small clusters is densely populated by local minima of potential energy with similar depth [2]. The structural fluctuation mentioned above has been interpreted as itinerancy among different local minima which is induced by deterministic chaotic motion going across the transition states [3]. Such *chaotic itinerancy* has been observed in a wide class of physical and biological systems [4]. Anomalous fluctuation inherent in clusters is a significant subject of few-body dynamics and nonlinear dynamics, which is beyond the traditional approach of statistical physics.

Recently Yasuda, Mori *et al.* have observed a very rapid alloying behavior in nanometer-sized metallic clusters such as Au–Cu system by *in situ* experiment with transmission electron spectroscopy [5]. Such a rapid alloying phenomenon seems to be a manifestation of the dynamical activity inherent in cluster systems. The main results of their extensive studies for various combinations of metallic species may be summarized as follows.

(a) The solute atoms deposited onto the host cluster dissolute into the host cluster at an anomalously rapid rate even at room temperature. Such a rapid alloying phenomenon is controlled by the heat of solution of the solute atom to the host metal: the rapid alloying occurs for a wide class of combinations of metals with negative heat of solution [6].
(b) Homogeneous dissolution of the solute atom into the host cluster occurs when the size of the cluster is less than a critical size. In clusters of size larger than the critical size, rapid alloying takes place only in shells around the surface of the cluster and a core occupied by the host metal is retained [7]. The critical size increases with the magnitude of the negative heat of solution [6].

Therefore, the spontaneous alloying seems to be a universal phenomenon which is observed in general for arbitrary combinations of metallic species with negative heat of solution.

Further by the observation that doubly twined clusters remain unchanged before and after the rapid alloying, they concluded that [8]

(c) the rapid alloying proceeds without melting in the sense that the global crystalline structure is not changed throughout the alloying process.

[a] JSPS Research Fellow, *present address:* Institute for Fundamental Chemistry, Takano-Nishihiraki-cho 34-4, Sakyou-ku, Kyoto 606-8103, Japan.
[b] *Present address:* Department of Physics, Kwansei Gakuin University, 1-1-155, Uegahara, Nishinomiya 662-0891, Japan.

The time scale of alloying is less than 1–10 s, which implies the diffusion rate is 10^{9-10} times larger than that of the corresponding bulk system. These distinct features strongly suggest the presence of some new mechanisms of mixing in the metallic clusters.

The present article reports the first attempt to investigate whether such a rapid alloying phenomenon can be described by classical dynamical simulations assuming quite simple interaction potentials among metal atoms. We stress that we make our model as simple as possible, since rapid alloying seems to be a universal phenomenon controlled by the heat of solution and does not depend upon the detailed features of the metallic species.

2 Model potentials

In the present analysis we do not consider the explicit change of the electronic structure behind the formation of metallic bonding. We suppose that all the features of metallic bondings can be described by certain classes of model potentials. There have been proposed several semi-empirical model potentials which may reproduce the main properties of bulk metals. A typical example is one derived from the so-called embedded atom method (EAM) [9]. It is a many-body potential, which includes the effect of the electronic structure in the metals. Indeed it succeeded in reproducing a number of equilibrium properties of bulk metals. However, it is not assured that the EAM works well in the description of the dynamics of alloying small clusters, where the fluctuation of interatomic distances is much more enhanced than in the bulk metals. In particular, a serious defect of the EAM from the viewpoint of the numerical simulation is that it contains many parameters to be fitted, which makes it hard to control the heat of solution to give a desired value. As summarized in (a) and (b) in the previous section, the heat of solution plays the key role in the spontaneous alloying process observed by Yasuda *et al.* In fact the spontaneous alloying is a quite universal phenomenon which is supposed to be controlled dominantly by the heat of solution. It seems to be unlikely that such a phenomenon sensitively depends upon the details of the model potential. We thus choose a model potential with which the heat of solution can be easily controlled rather than a model potential faithfully reproducing the equilibrium properties of the corresponding bulk metals. The model potentials we use here is the Lennard-Jones (LJ) potential and the Morse potential which are both typical examples of two-body potentials. The LJ potential and the Morse potential contain only a few parameters, and can be written as,

$$V_{ss'}(r) = \epsilon_{ss'} \left\{ \left(\frac{r_{ss'}}{r}\right)^{12} - 2\left(\frac{r_{ss'}}{r}\right)^{6} \right\} \quad \text{(LJ)} \tag{1}$$

$$V_{ss'}(r) = \epsilon_{ss'} \left\{ e^{-2a_{ss'}(r-r_{ss'})} - 2e^{-a_{ss'}(r-r_{ss'})} \right\} \quad \text{(Morse)} \tag{2}$$

where ss' specifies the species of the two interacting atoms, say A and B. To extract the role of the heat of solution we consider the following simplified situation: we suppose that the bond length $r_{ss'}$, and the decay rate of potential $a_{ss'}$ are the same for two species, *i.e.*, $r_{AA} = r_{BB} = r_{AB}$, $a_{AA} = a_{BB} = a_{AB}$. We further suppose $\epsilon_{AA} = \epsilon_{BB} \equiv \epsilon$, then the only free parameters of the model potentials are $\alpha = \epsilon_{AB}/\epsilon_{AA}$ in the LJ potential, and α and $\rho = a_{ss'}r_{ss'}$ in the Morse potential. The heat of solution per atom necessary for the formation of dilute alloy is then controlled by the single parameter α

$$\Delta H = z(1-\alpha)\epsilon, \tag{3}$$

where z is the number of nearest neighbor atoms. In the realistic situation, the radius of the atoms are, of course, slightly different. Our assumption $r_{AA} = r_{BB} = r_{AB}$, $a_{AA} = a_{BB} = a_{AB}$ is not correct, but the results of simulation indicate that such a difference does not result in noticeable effects, and we are allowed to take such a simplification.

We note that the two-body potential, however, does not explicitly take into account the bond-weakening effect, which may be a crucial in the alloying process. Let us consider a pair of bonded atoms. If a third atom comes close to them and attracts electrons from the pairing bond, then the bond may be weakened and it may become easier for one of the paired atoms to change its partner to the third atom. The above mechanism is a typical example of many-body effect which can not be taken into account by the two-body force. A simple model potential which emphasizes such effects of electron transfer among atoms and of the change of electronic features of bonding has also been proposed based upon Pettifor's theory of metallic bonding and will be presented in a forthcoming publication [10].

3 Preparation of initial conditions and evolution rules

The deposition of solute atoms on the cluster and the subsequent formation of bonding with the host atom generate the heat of condensation ϵ per bond. The released energy significantly raises the temperature of the cluster, but the excess heat in the cluster relaxes to the substrate on a time scale much shorter ($10^{-6\sim-4}$ s) than the time interval of deposition ($\sim 10^{-1}$ s) [11]. Thus the atoms landing successively on the host cluster are accumulated and condensed. When the number of solute atoms condensed on the host cluster exceeds a certain amount, a rapid dissolution of solute atoms in the host cluster will take place. Such a scenario is supported by the experimental observation that Au-cluster closely adhered to a Sb-cluster also exhibits spontaneous alloying [12]. From these considerations, we prepare the initial condition in the following two steps.

(1) First, a cluster of a single species, say A, with a closed shell structure *i.e.*, hexagonal cluster of triagonal lattice (2D) or cuboctahedral cluster of fcc lattice (3D), or with a nearly closed-shell structure is prepared.

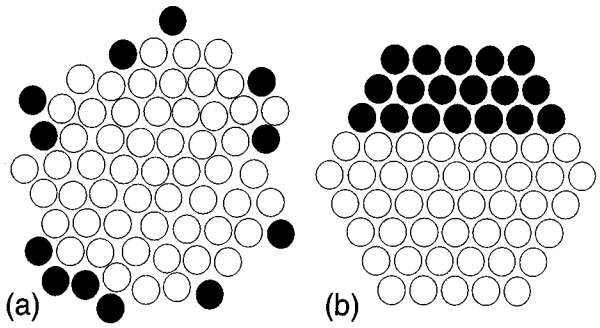

Fig. 1. Two typical initial spatial distributions of atoms used in our simulation. Open circles and filled circles indicate A- and B-atoms, respectively.

It is evolved with appropriate initial velocities until the excess potential energy is converted to the kinetic energy and the system reaches a quasi-equilibrium state.

(2) Then all atoms contained in a part of the cluster, or an appreciable number of atoms in outer shells of the cluster, are replaced by B-atoms.
The simulation starts with the same positions and momenta just before the replacement by B-atoms. We show in Figure 1 two different class of typical spatial configurations of initial conditions that we prepared.

With these initial conditions, we evolve the system by Hamilton's equation of motion using potentials (1, 2). Both 2D- and 3D-simulations were performed. In this article we confine ourselves to the 2D simulations, because the mixing process can easily be traced in 2D clusters, and moreover significant qualitative differences between 2D and 3D simulations has not been recognized yet.

As discussed above, the time scale on which the excess heat generated in the cluster relaxes toward the substrate is short compared to deposition, but rather ($10^{-6\sim-4}$ s) long compared to the time scale of alloying. This is attributed to the the fact that the coupling between the cluster and the substrate due to the Van der Waals force is much weaker than the metallic bonding. We first suppose that the major process of alloying completes within the time scale of heat relaxation. Accordingly time evolution of the system obeys the Hamilton's equation of motion

$$M_s \frac{dq_{si\ell}}{dt} = p_{si\ell}, \qquad \frac{dp_{si\ell}}{dt} = -\sum_{is,js'} \frac{\partial V_{ss'}(r_{isjs'})}{\partial q_{si\ell}}, \quad (4)$$

where p_{si}, q_{si} are the momentum and the coordinate of the $\ell(=x,y,z)$th component of the ith atom of the species s ($=A$ or B) with mass M_s. This simulation may be called "microcanonical" or "isoenergetic" simulation in which the total energy of the atoms is conserved.

Another extreme limit is that in which the isothermalization by the substrate is significant. For the isothermal condition it is reasonable to employ the evolution rule based on the Langevin equation, where the second equation of equation (4) is replaced by

$$\frac{dp_{si\ell}}{dt} = -\gamma p_{si\ell} - \sum_{is,js'} \frac{\partial V_{ss'}(r_{isjs'})}{\partial q_{si\ell}} + f_{si\ell}, \qquad (5)$$

which contains the friction force $-\gamma p_{si\ell}$ and the random force $f_{si\ell}$, which is δ-correlated, *i.e.*, $\langle f_{si\ell}(t) f_{si\ell}(t')\rangle = k_B T\gamma\delta(t-t')$, where T is the temperature. With this model, we can examine the effect of the isothermalization on the spontaneous alloying. The majority of the results shown in the next section is devoted to the isoenergetic simulation. In the last section we compare them with the results of the isothermal simulation.

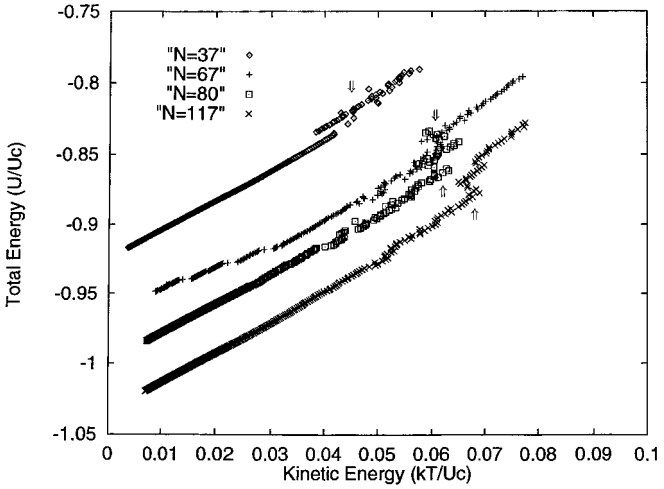

Fig. 2. Caloric curves (total energy *versus* kinetic energy) for typical Morse clusters: $N = 37$, $N = 67$, $N = 80$ and $N = 117$. The melting temperatures are decided by the hysteretic part indicated by the arrows.

4 Results

4.1 Case of $\alpha = 1$

We first discuss the case of $\alpha = 1$. In this case the cluster is effectively composed of a single species. As a result the rapid dissolution of B in A-cluster occurs only above the melting temperature T_M. Since the melting temperature is a quite important parameter in what follows, we discuss it rather in detail.

In the isoenergetic simulation we define the temperature T as the local time average of the total kinetic energy (E_{kin}) of the cluster with $NDk_BT/2 = \int_t^{t+\Delta t} E_{kin}(t')dt'/\Delta t$, where Δt is an averaging time taken much longer than the Debye period t_D (typically $\Delta t \sim 10^3 t_D$), D is the spatial dimension, and N is the number of atoms contained in the cluster. In small clusters melting does not occur homogeneously: the melting takes place on the surface at lower temperature and it proceeds in the inner shells as the temperature T rises.

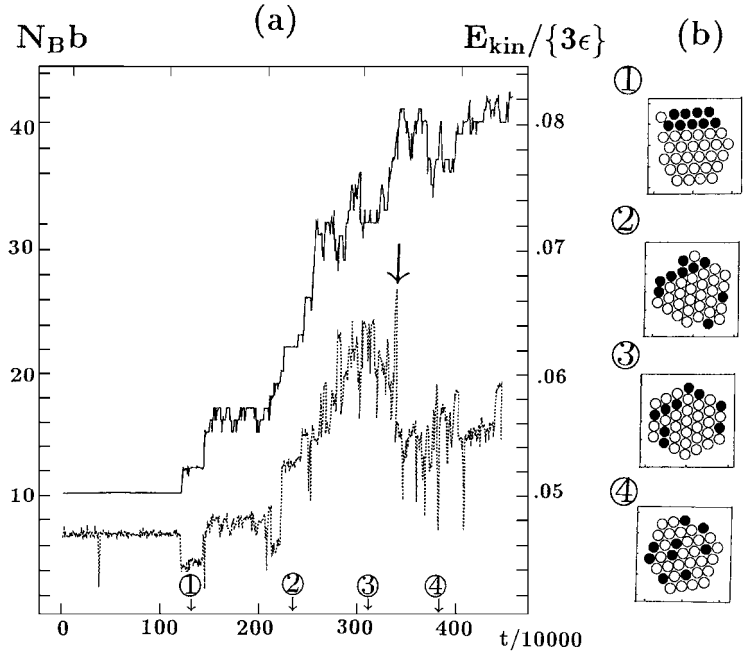

Fig. 3. (a) Time evolutions of the bond number $b(t)$ (solid line) and the kinetic energy E_{kin} per atom (dotted line) in the rapid alloying process of a 2D LJ cluster ($(N_A, N_B) = (28, 9)$, $\alpha = 1.2$), and (b) representative spatial distributions of A- and B-atoms in the four stages ①–④ discussed in the text. The times of the four patterns are indicated in (a).

Hereafter we define the melting temperature T_M as the temperature above which even the core part of the cluster melts. In practice, T_M is estimated by the caloric curve, *i.e.*, the relation between T and the total energy U, which is known to exhibit a hysteretic behavior close to T_M [2]. We show in Figure 2 typical examples of caloric curves for different sized 2D Morse clusters.

Above T_M the mixing among the two species occurs very rapidly, but the B-atoms which go into the inner shells occupied by the A-atoms often come back again to the surface, demonstrating that such a process is not a *unidirectional* alloying process but a *bidirectional* diffusion process. At well below T_M, the diffusion into the inner shells part is inhibited, and complete mixing between the two species can no longer be observed within the time scale accessible by computer simulation. But it should be emphasized that the surface melts even well below T_M in the sense that the atoms on the outer layer can diffuse along the surface. It is well-known that T_M decreases with the size of the cluster [13]. For typical clusters with the number of shells $m \sim 4$–6 $(30 < N = N_A + N_B < 120)$ the melting temperature is estimated as $k_B T_M/U_c \sim 0.050$–0.070 and ~ 0.045–0.070 for typical 2D LJ and Morse clusters, respectively, where $U_c = z\epsilon/2$ is the heat of condensation per atom.

Before closing this section, we stress again that even at temperatures lower than T_M the atoms on the surface of the cluster can diffuse along the surface.

4.2 Case of $\alpha < 1$

For two component clusters with positive heat of solution where $\alpha < 1$, the mixing between the two species is not observed, even if the initial temperature T_0 is far above the melting temperature T_M. For $T_0 > T_M$ the atoms rapidly exchange the positions with atoms of the same species, but the two species are separated with an interface, and do not mix with each other at all. That is, we cannot find any symptoms revealing onset of alloying in the cluster for $T_0 < T_M$ in our simulation.

4.3 Case of $\alpha > 1$

In this part we discuss the most interesting case where the heat of solution is negative *i.e.*, $\alpha > 1$. It takes extremely long CPU time to simulate with conditions corresponding to the actual experimental situations of the spontaneous alloying. To make the computation time short enough to be accessed by available computational resource, simulations are executed for heat of solution larger ($|\alpha| = 1.2$) than that of real systems ($|\alpha| = 1.02$ (Au−Cu)−1.07 (Au–Al)) and for initial temperature $T_0 > 2T_M/3$, which is higher than in actual experiments (*i.e.*, $T_0 \sim 300$ K $\sim T_M/3$). If the initial temperature T_0 is higher than the melting temperature T_M, the solute B-atoms condensed on the host A-cluster always dissolve into an alloyed cluster. The alloying rate is, however, significantly larger than the diffusion rate in case of the single component *i.e.*, $\alpha = 1$. The time scale of dissolution increases rapidly with decrease in T_0, but even for the initial temperature below T_M the alloying behavior can surely be observed.

To quantify the time evolution of the alloying process, we introduce the bond number $b(t)$ as the average number of nearest neighbor host (A) atoms to the solute (B) atoms.

$$b(t) = \sum_{i \in \{B-atoms\}} \frac{N_{A(i)}(t)}{N_B} \tag{6}$$

where $N_{A(i)}(t)$ is the number of nearest neighbor A-atoms around the ith B-atom at time t, and N_B is the total number of B-atoms.

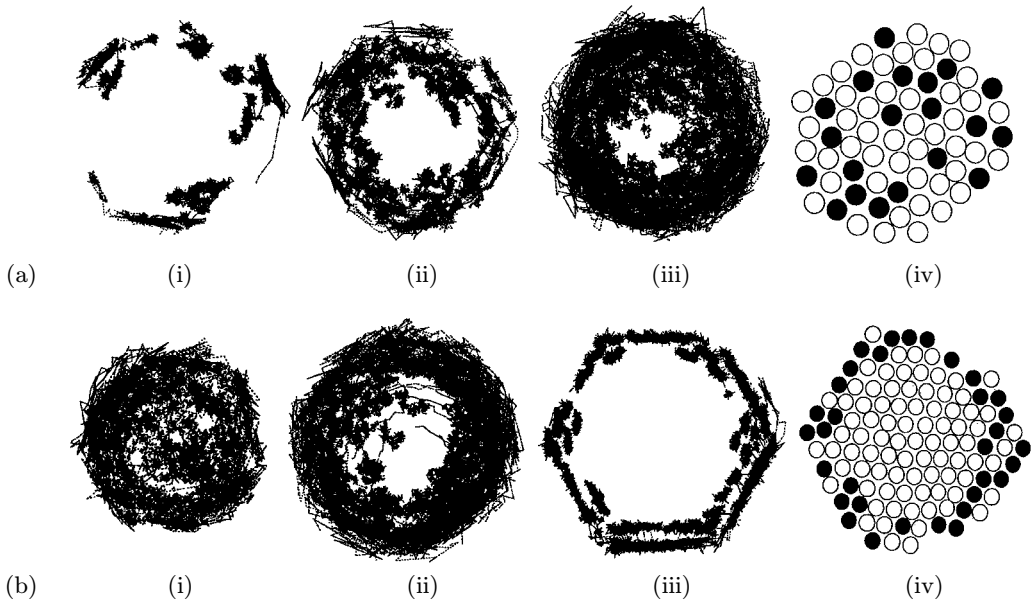

Fig. 4. The trajectories of position coordinates of all B-atoms in 2D Morse clusters: (a) $m = 5$ and r increases as (i) $r = 0.09$, $(N_A, N_B) = (61, 6)$, (ii) $r = 0.18$, $(N_A, N_B) = (55, 12)$ and (iii) $r = 0.3$, $(N_A, N_B) = (47, 20)$; (b) $r = 0.3$, and the cluster size increases as (i) $m = 4$ $(N_A, N_B) = (23, 9)$, (ii) $m = 6$ $(N_A, N_B) = (56, 24)$ and (iii) $m = 7$ $(N_A, N_B) = (84, 33)$. See the text.

Figure 3a shows a typical example of the time evolution of $b(t)$ together with the kinetic energy E_{kin} per atom, which are obtained for a 2D LJ cluster starting from the initial configuration of Figure 1b. The spatial configurations of the two species are also displayed in (b). The bond number $b(t)$ increases monotonically with the value of the bond number for homogeneous mixing $b_h = z(1-r)$. This directional relaxation of $b(t)$ is quite different from the diffusive relaxation process observed in the $\alpha = 1$ cluster, where $b(t)$ fluctuates and a monotonic increase is not observed. The whole process consists of the following stages: ① the surface diffusion is initiated, ② the clustered B-atoms collapse and surround the A-host, ③ the B-atoms enter into the host cluster being enclosed by the A-atoms, and ④ the B-atoms are mixed strongly with the A-atoms and the alloying completes.

As shown in Figure 3a the kinetic energy increases in the stage ③ and saturates at the level of T_M in ④. In the stage ④ some atoms dissociate from the cluster (very often from the 2D LJ cluster, but not very often from the 3D LJ and the 2, 3D Morse cluster). Then, as indicated by an arrow, the kinetic energy suddenly decreases and the cluster cools down.

Such a rapid and homogeneous alloying can not occur if the relative ratio r of the number of B-atoms to the total number of atoms in the cluster is not very large. Figure 4a shows the trajectories of the position coordinates of B-atoms starting from the initial configuration shown in Figure 1a on the same time scale numerically accessible, *i.e.*, $t \sim 10^5 t_D$. The Morse potential ($\alpha = 1.2, \rho = 3.68$) is used, and the initial temperature T_0 is fixed to the same temperature $k_B T_0/U_c = 0.051$ slightly lower than $k_B T_M$ ($\sim 0.060 U_c$). The number of shells of the cluster is taken as $m = 5$, and the total number of atoms is $N = N_A + N_B = 67$. The ratio r is increased in the order of (i) 0.09, (ii) 0.18 and (iii) 0.30 in Figure 4a, and (iv) shows a typical spatial distribution of (iii) in the final stage. It is evident that as the ratio increases, the maximal depth which B-atoms can finally reach increases, and in (iii) some B-atoms can reach in the center of the cluster. This fact implies that cooperative action among the solute atoms is crucial for homogeneous alloying to take place.

On the other hand, as the size of cluster increases, the homogeneous alloying becomes suppressed. We show in Figure 4b how the process of mixing into the inner shells changes as the cluster size is increased. Morse clusters starting from the same initial temperature as in Figure 4a are examined. In (i), (ii) and (iii), the ratio r is fixed to the same value as Figure 4a (iii), (where $m = 5$) and m is increased as $m = 4, 6$ and 7, respectively. A typical spatial distribution of (iii) in the final stage is depicted in (iv). It is evident that the mixing is homogeneous if $m \leq 5$, but as m is increased further, the alloyed region is localized closer to the surface. If m is larger than 7, the B-atoms can no longer enter into the inner shells. These results show that the homogeneous alloying in the smaller sized clusters ($m \leq 5$) occurs much more rapidly than in the corresponding bulk. Numerically, we confirmed that the critical shell number of the *rapid homogeneous* alloying increases if the the parameter α, which controls the heat of solution, is increased. It should be noted, however, that the stages ① and ②, which initiate the following rapid alloying process, are due to the easiness of atomic motion close to the surface. Therefore, roughly speaking, the rapid alloying occurs in such a cluster when the number of surface atoms overwhelms the number of the remainder, *i.e.*, in clusters of $m \leq 4{-}6$ for 2D and of $m \leq 10{-}12$ for 3D.

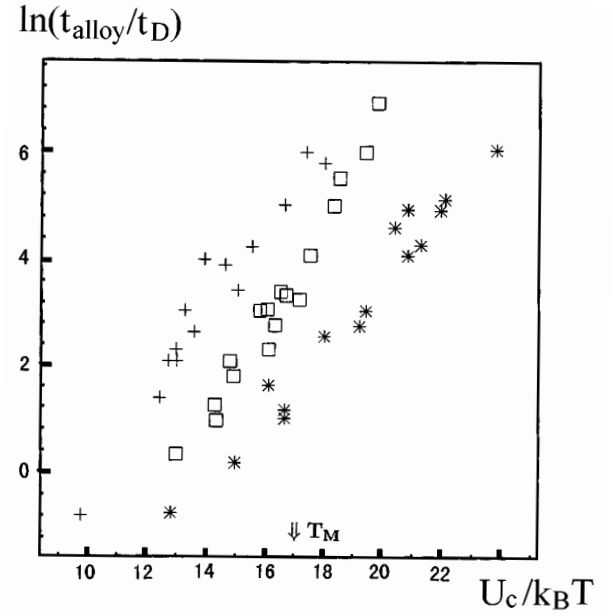

Fig. 5. Dependence of the alloying time t_{alloy} on the initial temperature T_0 for a typical 2D LJ-cluster ($(N_A, N_B) = (28, 9)$ and initial condition Fig. 1a); (+): isoenergetic (microcanonical) simulation, (∗): isothermal (Langevin) simulation for the cluster of $\alpha = 1.2$, and (□): isoenergetic simulation for the cluster of $\alpha = 1$.

Finally we estimate the time scale of such a "rapid" alloying at room temperature. As stated above, our simulation is done at initial temperature ($T_0 > 2/3T_M$) higher than room temperature ($T_0 \sim T_M/3$), and as shown in Figure 5, the alloying times obtained for a typical 2D LJ cluster ($N_A = 28, N_B = 9$ and the initial condition of Fig. 1a) obeys an Arrhenius-like law in such a temperature regime. In fact, the semi-log plot of the alloying time t_{alloy}, which is defined as the time when $b(t)$ reaches $(b(0) + b_h)/2$, *versus* the inverse of the initial temperature T_0 is a straight line, which yields the empirical rule

$$t_{alloy} \sim a t_D e^{E_{alloy}/T_0 k_B}, \tag{7}$$

where the activation energy E_{alloy}/U_c and the constant a are fitted to 0.615 and 2.0×10^{-4}, respectively. Extrapolating the rule to room temperature, we can estimate the alloying time, for example, $t_{alloy} \sim 10^9 t_D$ and $t_{alloy} \sim 10^{12} t_D$ at $T_0 \sim 300$ K for $\epsilon = 0.40$ eV (which gives $T_M = 930$ K) and $\epsilon = 0.5$ eV ($T_M = 1160$ K), respectively. This implies $t_{alloy} \sim 10^{-4}$–10^{-1} s for $t_D \sim 10^{-13}$ s, which is a reasonable time scale consistent with experiment. Similar behavior has been observed also for the Morse cluster, but the activation energy E_{alloy} is significantly smaller than for the LJ cluster. For comparison, we have shown the plots of t_{alloy} *versus* T_0 in the case of $\alpha = 1$. These plots are also straight lines. However, the slope of the plots is much larger than in the case of $\alpha = 1.2$: E_{alloy}/U_c and the constant a are estimated to be 1.42 and 2.8×10^{-9}, respectively. The present estimation yields an extremely long time scale $t_{alloy} \sim 10^7$–10^{14} s at room temperature.

The 2D-EAP cluster and the 3D-Morse cluster also exhibit similar rapid alloying processes, which will be presented in detail elsewhere [14].

5 Discussion

The results mentioned above agree quite well with the experimental results summarized as (a) and (b) in Section 1. However, the presence of the final stage ④ in the LJ cluster seems to be somehow inconsistent with the experimental conjecture (c) that the whole of the alloying process proceeds without melting. In fact, the melting of the cluster is observed also in the Morse clusters shown in Figure 4a and 4b. This is because our simulation is microcanonical and the total energy is conserved, which results in the heating up of the cluster due to the emission of the reaction heat. The temperature reaches the maximum value as the ideal mixing is achieved. The maximal increment of temperature ΔT is estimated to be $\Delta T \sim 2r(1-r)(\alpha-1)U_c/k_B$ in the large limit of the cluster size. It is significant at the value $\alpha = 1.2$ taken in the simulations so far discussed, because the initial temperature was not set much lower than T_M.

However, if we are allowed to take smaller values of α, T_0 and r, the temperature may be kept below T_M even if homogeneous mixing takes place. Such a simulation takes a very long CPU time, and we have examined only a few examples under such conditions, but we have some evidence showing that the solute atoms dissolute without the melting of the cluster. Figure 6a shows a typical example. In this example we used a Morse cluster of $N = 67$ ($(N_A, N_B) = (55, 12)$) and $\alpha = 1.1$ starting with the initial condition of Figure 1b. The initial temperature is chosen to be $T_0 = 0.042U_c/k_B \sim 0.71T_M$. It is clear that an almost homogeneous alloying is achieved in the final stage. The positions of individual atoms are exchanged and so the crystal axis slightly rotates, but the hexagonal structure of the cluster remains unchanged throughout the whole process of the rapid alloying. Indeed, as shown in (b) the rise of the temperature is small, and the temperature is kept well below T_M. Moreover, the substrate, which is not taken into account in our simulation, will absorb the excess heat and enable rapid alloying without rise of temperature.

On the other hand, isothermalization effect by the substrate suppresses the rapid alloying process. To investigate the effect of isothermalization due to the contact with the substrate, we show in Figure 5 the plot of t_{alloy} *versus* T_0 obtained by using the Langevin equation (5). The friction constant γ was chosen to be much larger (typically to the order of t_D^{-1}) than the actual value in order to emphasize the effect of the isothermalization. It is evident that the effective activation energy estimated by the slope of the Arrhenius plot is significantly larger than the isoenergetic simulation. It is estimated as $E_{alloy}/U_c \sim 0.82$,

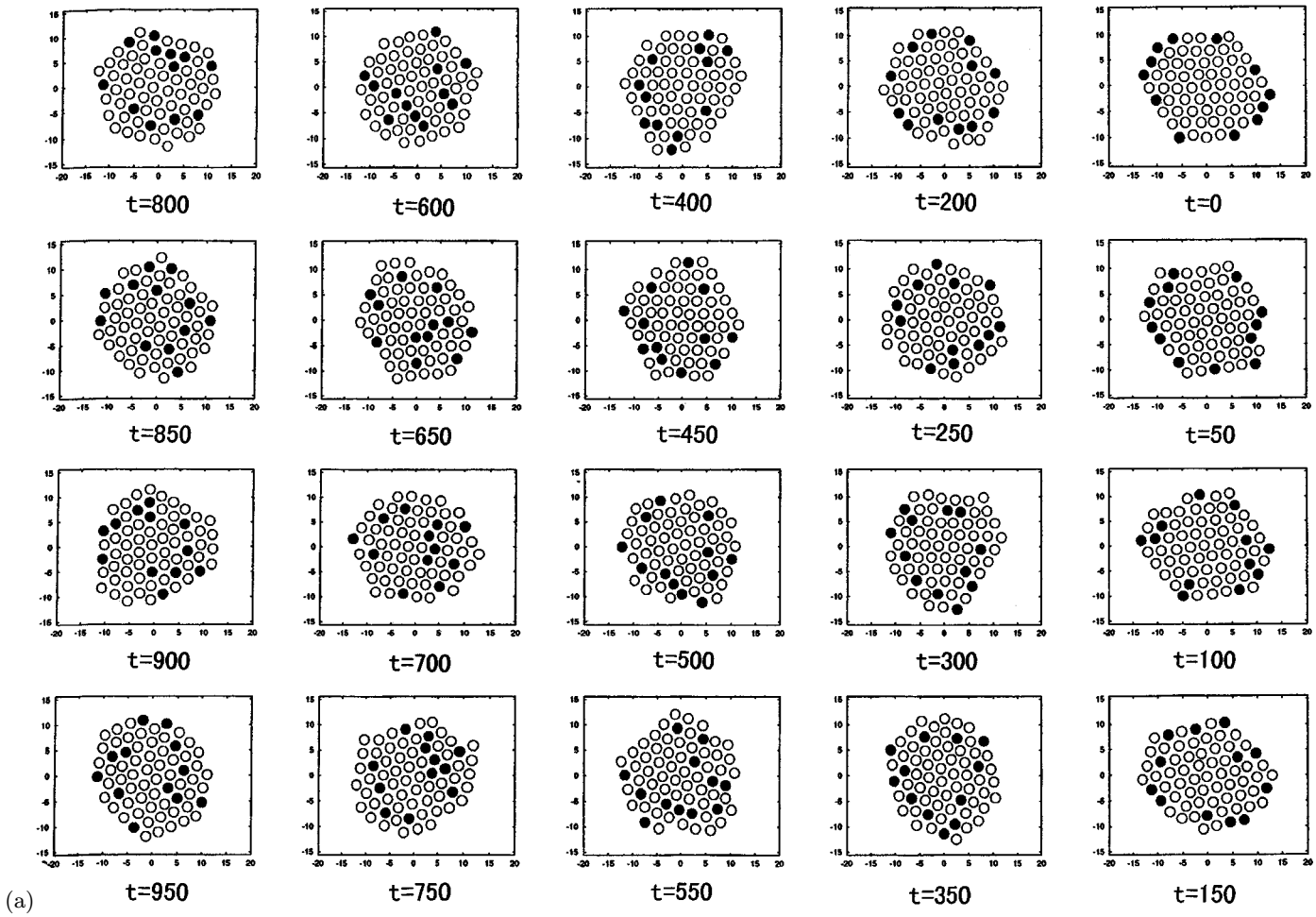

(a)

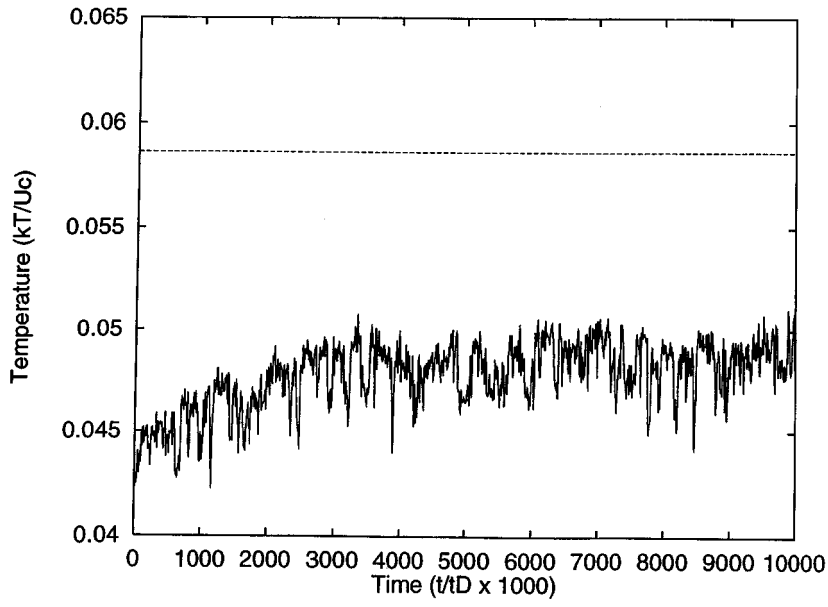

(b)

Fig. 6. (a) Time evolution of the alloying process of the Morse cluster shown in Figure 4a, where t indicates time (ns), where $t_D = 10^{-13}$ s, and (b) the evolution of the temperature T. The broken line is the melting temperature determined from the caloric curve (Fig. 2).

and $a \sim 4.0 \times 10^{-4}$. From an extrapolation to room temperature of the Arrhenius plot one can evaluate the alloying time $t_{alloy} \sim 1 - 10^4$ s which is 10^4 times longer than in the isoenergetic simulation. The above results imply that too strong coupling with the heat reservoir severely suppresses the rapid alloying process. The weakness of the coupling with the substrate will be a necessary condition for the occurrence of the rapid alloying.

Summarizing the above observations we can conclude that rapid alloying certainly can occur without melting of the cluster. The alloying rate will be maximal in the isoenergetic condition. Even if coupling with the substrate exists, rapid alloying can be achieved, provided that the absorption of the excess heat by the substrate occurs slowly enough. Further systematic investigations are now in progress. The details will be presented in forthcoming publications [14]. The most interesting theoretical problem unclarified yet is what kind of dynamical process is responsible for the rapid alloying observed here.

The authors are very grateful to H. Yasuda and H. Mori for fruitful discussions. They are indebted to C. Satoko for his suggestion of the two-body potential simulation. We also thank P. Davis for useful advices in preparing the present manuscript. This work is supported by a Grant-in-Aid on Priority Areas, "Chemistry of Small Manybody System", from the Ministry of Education, Science, and Culture, Japan. One of the authors (Y.S.) thanks financial support from Grant-in-Aid for JSPS fellows.

References

1. J.O. Bovin, R. Wallenberg, D.J. Smith, Nature **317**, 47 (1985); S. Iijima, T. Ichihashi, Phys. Rev. Lett. **56**, 616 (1986); M. Mitome, Y. Tanishiro, K. Takayanagi, Z. Phys. D **12**, 45 (1989); P.M. Ajayan, L.D. Marks, Phys. Rev. Lett. **63**, 279 (1989).
2. R.S. Berry, Chem. Rev. **93**, 2739 (1993) and references cited therein.
3. S. Sawada, S. Sugano, Z. Phys. D **14** (1989) 247; S. Sawada, S. Sugano, Z. Phys. D **24**, 377 (1992).
4. See, for example, K. Ikeda, *Proc. of Int. Symp. on Information Physics*, edited by I. Tsuda, K. Takahashi (Kyushu Institute of Technology, 1992), p. 101 and references cited therein.
5. H. Yasuda, H. Mori, M. Komatsu, K. Takeda, H. Fujita, J. Electron Microsc. **41**, 262 (1992).
6. H. Yasuda, H. Mori, Phys. Rev. Lett. **69**, 3747 (1992); H. Yasuda, H. Mori, Intermetallics **1**, 35 (1993); H. Yasuda, H. Mori, T. Muraki, T. Sakata, Z. Phys. D **31**, 209 (1994); H. Mori, H. Yasuda, J. Microsc. **180**, 33 (1995).
7. H. Yasuda, H. Mori, Z. Phys. D **31**, 131 (1994).
8. H. Mori, H. Yasuda, T. Kamino, Phil. Mag. Lett. **69**, 279 (1994).
9. M.S. Daw, M.I. Baskes, Phys. Rev. B **29**, 6443 (1984); S.M. Foiles *et al.*, Phys. Rev. B **33** 7983 (1986).
10. S. Sawada, K.S. Ikeda, Y. Shimizu (in preparation).
11. H. Yasuda (preprint and private communication).
12. H. Yasuda, H. Mori, Z. Phys. (in press).
13. Ph. Buffat, J.-P. Borel, Phys. Rev. A **13**, 2287 (1976).
14. Y. Shimizu, S. Sawada, K.S. Ikeda (in preparation).